



ISSN: 2723-9535

Available online at www.HighTechJournal.org

HighTech and Innovation Journal

Vol. 5, No. 2, June, 2024



Prediction of Dust Emissions in Highway Subgrade-Filling Construction Based on Deep Neural Network

Zhibin Wang¹, Lei Feng¹, Yanwei Li¹, Qunle Du², Lin Zhao³, Xingju Wang^{3*} 

¹Taihang Urban and Rural Construction Group Company Limited, Hebei Province, 050200, China.

²Hebei Expressway Development Group Company Limited, Hebei Province, 050899, China.

³Shijiazhuang Tiedao University, Hebei Province, 050043, China.

Received 15 February 2024; Revised 19 May 2024; Accepted 26 May 2024; Published 01 June 2024

Abstract

Dust pollution can harm the urban environment and the health of citizens. Each stage in highway construction generates unorganized dust emissions to varying degrees, which complicates their quantification. To precisely forecast dust emissions during the construction of highway subgrades and reduce the associated pollution risks, this study introduces a predictive model based on a deep neural network (DNN) for dust emissions during highway subgrade-filling operations. Dust concentration is treated as a nonlinear multivariate problem, with predictive indicators encompassing particulate matter 2.5 (PM_{2.5}), particulate matter 10 (PM₁₀), ground surface temperature, wind speed, air temperature, surface pressure, and relative humidity. Using a DNN model, this study forecasts the concentrations of PM_{2.5} and PM₁₀ at highway construction sites. Based on a highway project in Hebei Province, this study predicts dust-emission concentrations via field monitoring conducted using self-developed equipment. The model's predictions exhibit a small mean-absolute-percentage error and root-mean-square error compared with the actual values, and the model's accuracy significantly surpasses that of conventional regression models. Accurate forecasting can facilitate the timely control of dust concentrations at construction sites, thus facilitating more environmentally friendly and efficient construction.

Keywords: Highway Engineering; Subgrade Filling; Dust Prediction; DNN.

1. Introduction

Highway transportation significantly affects the development of the national economy and daily life. In recent years, the construction of expressway networks in China has accelerated, with the total mileage of highways increasing annually. According to statistics from the Ministry of Transport, the total length of expressways nationwide reached 535,000 km by the end of 2022 [1]. However, large-scale construction of expressways inevitably generates substantial amounts of construction dust. Therefore, construction dust has contributed significantly to excessive atmospheric particulate matter concentrations in recent years [2]. Prolonged human exposure to environments with excessive particulate-matter concentrations can result in diseases to the skin [3], respiratory system, and cardiovascular system [4–6], thereby damaging health and resulting in economic and property losses. Therefore, the concentration of construction dust must be predicted and controlled to mitigate its impact on the environment and human health.

* Corresponding author: wangxingju@stdu.edu.cn

 <http://dx.doi.org/10.28991/HIJ-2024-05-02-03>

➤ This is an open access article under the CC-BY license (<https://creativecommons.org/licenses/by/4.0/>).

© Authors retain all copyrights.

In recent years, researchers have extensively investigated construction dust, including topics such as dust-monitoring techniques [7], dust emission factors [8, 9], dust dispersion [10–12], dust-pollution characteristics [13, 14], health-hazard assessments [15–17], and dust-control measures [18].

Instrumental sampling is the most commonly used method for monitoring the concentration of construction dust. Gao et al. [19] employed an HXF35 dust sampler to measure the concentration of total suspended particulates. To address the complexity and uniqueness of construction sites, Ma et al. [20] designed an automatic monitoring system for construction-dust pollution sources using unmanned aerial vehicles and image recognition technology. Construction dust was analyzed from three perspectives: detection of construction-dust pollution sources, identification of construction-dust pollution areas, and comparison of characteristics of construction-dust pollution sources.

In terms of fugitive-dust emission factors, numerous researchers have considered the relationship between fugitive-dust emissions and major gaseous pollutants such as NO_x and SO_x . Liu et al. [21] employed the land-use regression model to elucidate the correlation and spatial variation between $\text{PM}_{2.5}$ and NO_2 in Shanghai, China. By analyzing data from multiple monitoring sites, Eeftens et al. [22] identified a generally high correlation between NO_2 and $\text{PM}_{2.5}$ absorbance. Recently, researchers investigated the relationship between fugitive-dust pollutants and meteorological factors. Using 11 years (1998–2008) of continuous observational data from the contiguous United States, Tai et al. [23] applied the multiple linear regression (MLR) model to demonstrate a robust correlation between $\text{PM}_{2.5}$ and meteorological factors. Pateraki et al. [24] investigated the effects of meteorological conditions on particles of different diameters (PM_{10} , $\text{PM}_{2.5}$, and $\text{PM}_{2.5-10}$) in cities surrounding the Mediterranean and confirmed a close relationship between high concentrations of PM_{10} and $\text{PM}_{2.5-10}$ and the local southwesterly wind regime. Zhang et al. [25] discovered that relative humidity and sunshine hours were most closely associated with $\text{PM}_{2.5}$. Zhang et al. [26] performed a multifractal asymmetric detrended cross-correlation analysis to discuss the cross-correlations between $\text{PM}_{2.5}$ concentrations and meteorological factors such as temperature, air pressure, relative humidity, and wind speed in Beijing and Hong Kong. They reported that the cross-correlations between $\text{PM}_{2.5}$ concentrations and these four meteorological factors exhibited multifractal and anti-persistent characteristics.

Additionally, researchers have extensively investigated the forecasting of construction dust concentration. To establish predictive models for construction dust emissions, researchers have used conventional MLR models [27–28]. Linear regression models are advantageous owing to their computational simplicity and minimal data requirements. However, they present significant limitations in capturing the relationship between the concentration of dust-emission particles and the monitoring factors of dust emissions, thus resulting in less accurate predictions. Subsequently, the autoregressive integrated moving average model (ARIMA) [29], which is based on an MLR model and integrates autoregressive and moving averages, is used for monitoring and forecasting. This model considers seasonal variations in the study subjects and can effectively predict linear data. However, its predictive accuracy is relatively low in nonlinear cases.

Aided by the advancement and proliferation of computer technology, researchers have addressed the disadvantages of regression models in fugitive dust forecasting by applying several machine learning methods to mitigate environmental issues caused by air pollution and construction dust. The most commonly used predictive methods include artificial neural networks (ANNs) [30], recurrent neural networks [31], convolutional neural networks (CNNs) [32, 33], and long short-term memory (LSTM) neural networks [34, 35]. ANNs are among the most commonly used models for forecasting fugitive-dust concentrations. Wang et al. [36] and Araújo et al. [37] employed ANN models to estimate the health risks associated with air pollution and predict the daily concentrations of $\text{PM}_{2.5}$. Karacan [38, 39] and Mathatho et al. [40] utilized ANNs to predict and optimize hazardous-substance concentrations in specific operational environments. Park et al. [41] proposed an ANN model to measure PM_{10} concentrations in large urban areas, which achieved a value that was 60% to 80% of the actual values. In addition to ANNs, dust-pollution forecasting models based on LSTM networks have demonstrated superior performance compared with other conventional models, such as ARIMA and support vector regression [42]. For instance, Li et al. [43] attempted to integrate LSTM with quadratic decomposition and optimization algorithms to establish a hybrid model for air quality index forecasting. Furthermore, to enhance model accuracy, researchers have begun to investigate the combination of multiple deep-learning networks [44, 45]. The highly regarded CNN-LSTM model combines the advantages of CNNs and LSTM. CNNs can effectively extract features from grid data, whereas LSTM exhibits excellent processing capabilities for time-series data. For example, the CNN-LSTM model designed by Huang et al. for forecasting $\text{PM}_{2.5}$ in smart cities uses features extracted by CNNs and analyzed by LSTM [46]. Compared with standalone LSTM models, hybrid forecasting models based on CNN-LSTM exhibit significantly lower errors [47].

Theories and practical applications pertaining to fugitive-dust monitoring equipment, monitoring factors, and forecasting methods have been extensively investigated. However, issues remain, such as the insufficient frequency of

data updates from monitoring equipment, the incomplete consideration of monitoring factors, and the necessity for improving forecasting models. In the existing fugitive-dust forecasting models, MLR models cannot readily capture the relationship between the concentration of fugitive-dust emission particles and the monitoring factors. Although machine learning models such as ANNs, CNNs, and LSTM networks can improve the accuracy of forecasting results, they present certain issues in nonlinear modeling and require a long time for model training. Deep neural network (DNN) models [48, 49] offer a distinct advantage in nonlinear modeling that facilitates the establishment of nonlinear predictive models capable of accurately reflecting the relationship between fugitive dust concentrations and monitoring factors. As such, they are extremely beneficial in enhancing the accuracy of forecasting outcomes.

To accurately predict the concentration of fugitive dust emissions during the roadbed filling phase of highway construction, this study focuses on forecasting PM2.5 and PM10, which are key indicators of dust emissions. By referring to previous studies pertaining to dust monitoring factors, we select surface temperature, wind speed, air temperature, surface pressure, and relative humidity as meteorological factors for dust monitoring, in addition to concentrations of PM2.5 and PM10 from the preceding moment as auxiliary influencing factors to synthesize indicators for dust concentration forecasting. Considering a highway construction site in Hebei as the experimental scenario, we use a self-developed dust-monitoring data-acquisition system to obtain data at 1-minute intervals. Based on the acquired monitoring data, we establish a DNN model to predict the concentrations of construction dust emissions in a specific environment. A flowchart of this study is shown in Figure 1.

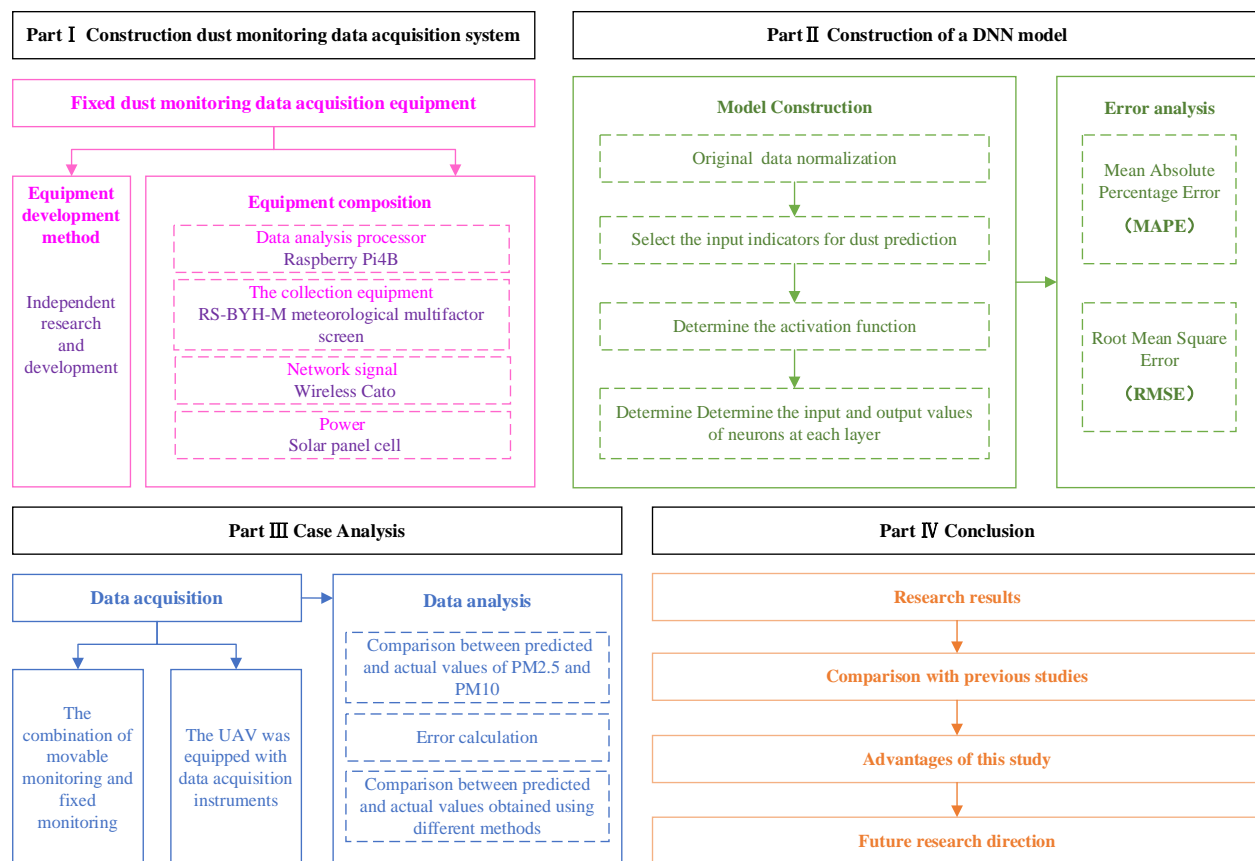


Figure 1. Framework for predicting construction dust based on DNN

2. Construction-Dust Monitoring Data-Acquisition System

Air-pollutant concentrations of PM2.5 and PM10 were obtained during the daytime from October to November 2020. The weather conditions, temperature, and other conditions were stable during the data-acquisition period.

An indigenously developed device was used for data acquisition, as shown in Figure 2. A Raspberry Pi4B (Raspberry Pi) was used as the data-analysis processor, and SDS011 was used as a high-precision laser PM2.5 sensor for environmental monitoring. Based on the network signal provided by the wireless system Cato, the data was uploaded to a self-developed Alibaba Cloud server for data storage.

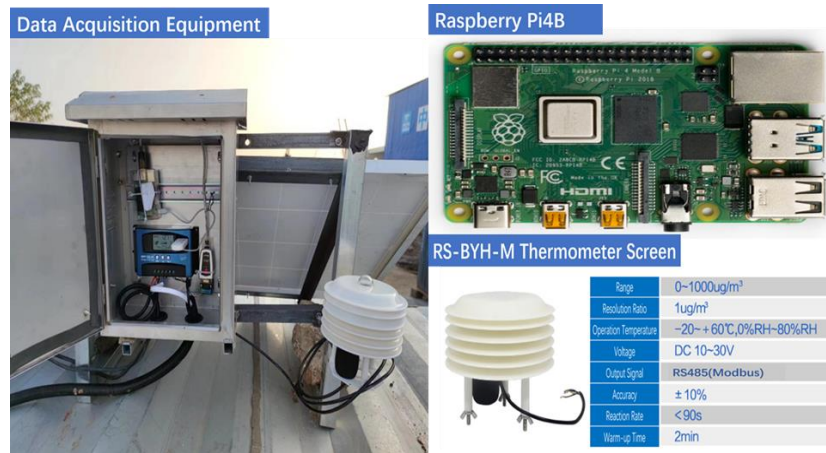


Figure 2. Fixed data-acquisition equipment

A Raspberry Pi processor was used for data analysis, as shown in Figure 2. The Raspberry Pi is a single-chip microcomputer that includes central processors, random-access memory, read-only memory, various input/output interfaces, interrupt systems, timers/counters, and other functions. We used a fourth-generation Raspberry Pi with a BCM2711 processor.

The acquisition equipment used was the RS-BYH-M meteorological multifactor screen, which integrates several environmental detection functions, including noise acquisition, PM2.5 and PM10 particle concentrations, temperature and humidity, atmospheric pressure, and light. A screen was installed in a louver box, the standard MODBUS-RTU communication protocol was used, and RS485 signals were output. The measured results showed that the maximum communication distance of the device was 2000 m. This transmitter is suitable for various applications, including ambient temperature and humidity measurements, noise monitoring, air quality detection, and atmospheric pressure and light intensity measurements.

The device was powered by a solar panel cell comprising solar elements of a specific size connected to form an efficient energy panel. The solar controller is the core control component of the photovoltaic power-supply system and manages the operation state of the entire system. The main functions of the solar controller include overcharging and discharge protection for the battery and load control voltage for voltage-sensitive devices. Through these controls and adjustments, the solar controller ensures the stable operation of the entire system and maximizes the use of solar energy resources.

3. Construction of DNN Model

3.1. Model Construction

A DNN offers excellent nonlinear processing capability owing to its compact and efficient nonlinear mapping structure. It features one input layer, multiple hidden layers, and one output layer, and it can manage significant amounts of data and complex features. Implementing more hidden layers results in a more complex model, better nonlinear characteristics, and richer features to be learned. The characteristics of a DNN are shown in Figure 3.

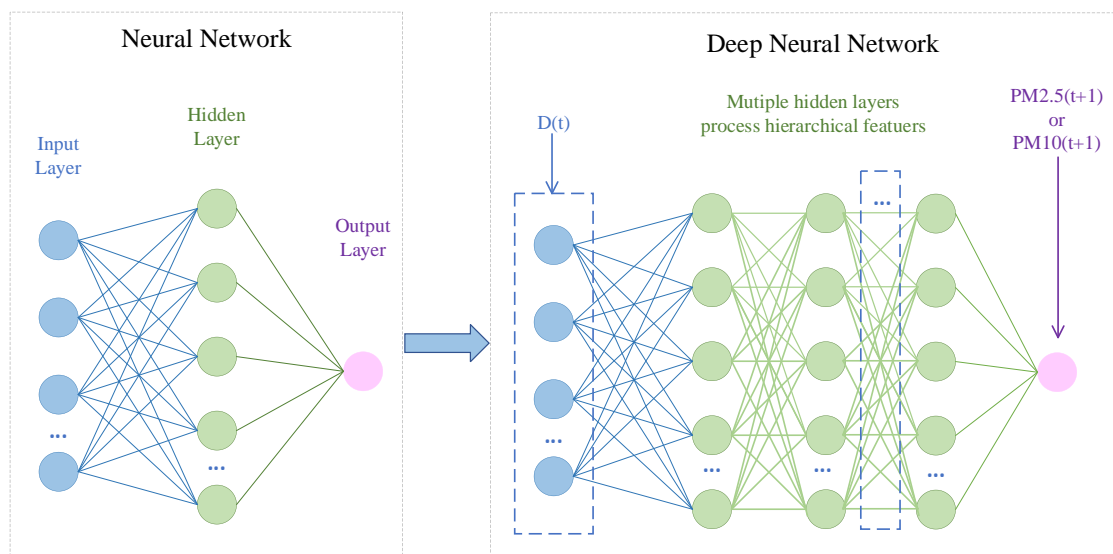


Figure 3. Characteristics of deep neural network

The input layer of a neural network inputs dust and environmental data at time t . Subsequently, the output layer outputs the predicted values of PM2.5 or PM10 at time $(t+1)$. In Figure 3, $D(t)$ is the input factor at time t , and $PM2.5(t+1)$ and $PM10(t+1)$ are the predicted values of PM2.5 or PM10 at time $(t+1)$, respectively. The correspondence between the input layer of the DNN and the dust monitoring indicators is listed in Table 1.

Table 1. Input indicators for dust prediction

Input Node	Indicator Name
X1	PM2.5
X2	PM10
X3	Surface temperature
X4	Wind speed
X5	Air temperature
X6	Surface pressure
X7	Relative humidity

The different layers of a DNN are fully connected; that is, any neuron in layer i is compulsorily connected to a neuron in layer $i+1$. If the input layer of the model contains n neurons, then the input of the k th neuron x_k can be expressed as

$$a_k^l = x_k \tag{1}$$

If layer $l-1$ contains m neurons, then the output a_k^l for the j th neuron in the first layer l can be expressed as

$$a_j^l = f \left(\sum_{k=1}^m w_{jk}^l a_k^{l-1} + b_j^l \right) \tag{2}$$

where f is the activation function in the hidden layer and a linear transfer function is used in the output layer. In the model, w is the connection weight and b is the offset; if $l = 2$, then a_i^l corresponds to the input layer x_k .

In this model, *RELU* was used as the activation function, as shown in Equation (3).

$$RELU(x) = \begin{cases} x, & x > 0 \\ 0, & x \leq 0 \end{cases} \tag{3}$$

where x denotes the corresponding input.

To facilitate rapid convergence during neural-network training, the original data were normalized. Considering the requirements of the neural-network algorithm for eigenvalue quantization, min–max normalization was adopted for the actual data.

$$x = \frac{x' - \min(x')}{\max(x') - \min(x')} \tag{4}$$

where x' represents the original data, x the air-quality data after processing, $\min(x')$ the minimum value for the same type of indicator data, and $\max(x')$ the maximum value for the same type of data.

3.2. Error Analysis

The universality and accuracy of the prediction models must be verified. Statistical indicators, including the mean error (ME), standardized mean deviation (NMB), mean-absolute-percentage error (MAPE), root-mean-square error (RMSE), and correlation coefficient (R), are typically used for error analysis. In this study, the MAPE and RMSE were selected for error analysis.

(1) The MAPE can be calculated as follows:

$$MAPE = \frac{1}{N} \sum_{i=1}^N \frac{|y_i^* - y_i|}{y_i} \times 100\%, \tag{5}$$

where y_i is the actual value of the i th sample, y_i^* the predicted value of the i th sample, and N the total number of predicted values.

(2) The RMSE can be calculated as:

$$RMSE = \sqrt{\frac{1}{N} \sum_{i=1}^N (y_i^* - y_i)^2} \tag{6}$$

where y_i is the true value of the i th sample; y_i^* is the predicted value of the i th sample; and N is the total number of predicted values.

4. Case Analysis

4.1. Data Acquisition

Considering a highway project in Hebei as an example, real-time monitoring of relevant data at the construction site was conducted using fixed construction dust monitoring equipment, as shown in Figure 2, and the portable monitoring equipment shown in Figure 4, which was utilized to supplement unclear or missing monitoring data from the fixed equipment.

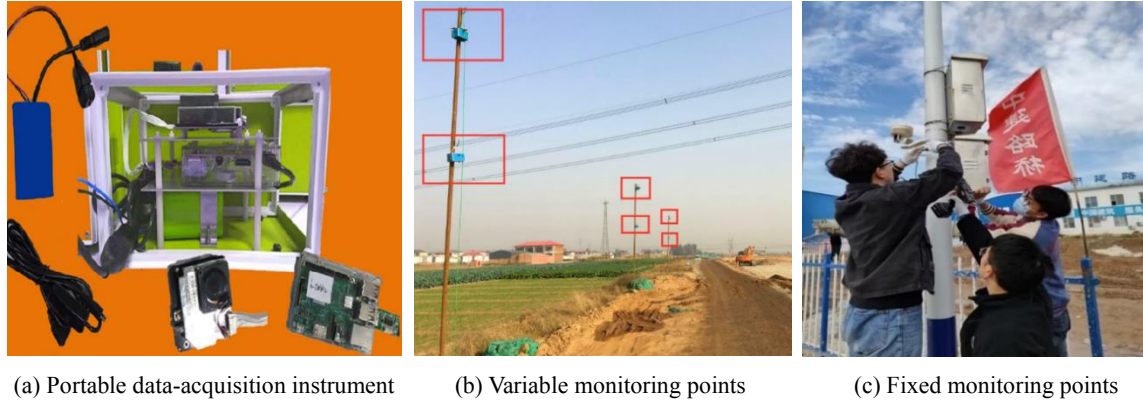


Figure 4. Installation of equipment at construction site

Considering safety, an application-oriented professional unmanned aerial vehicle (UAV, DJI M600 Pro, China) was used to conduct field explorations and comprehensive analyses of the topography, ground facilities, and airspace of the construction areas. The UAV can be equipped with data-acquisition instruments, as shown in Figure 4, which are designed to obtain PM2.5 and PM10 concentration data at a relative altitude of 100 m above the ground, as shown in Figure 5.



Figure 5. UAV equipped with portable data-acquisition instrument for data acquisition

Data were obtained on five days between October and November, from 10:00 to 15:00. The monitoring data included 1500 data points. The data obtained from the highway construction dust monitoring equipment is listed in Table 2.

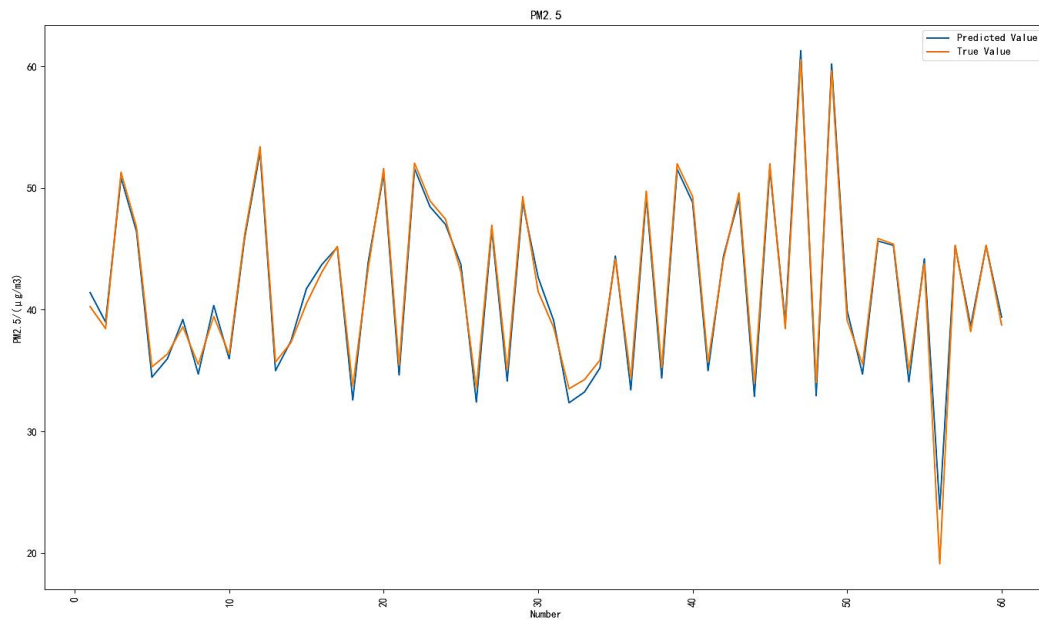
Table 2. Partial monitoring data of highway construction-dust monitoring equipment

Number	PM2.5	PM10	Surface Temperature (°C)	Wind Speed ($m \square s^{-1}$)	Air Temperature (°C)	Surface Pressure (hPa)	Relative Humidity (%)	Time
1	69.8	123.5	10.4	1.03	13.1	1024.00	57.7	2020-10-29 10: 00
2	71.3	143.6	10.4	1.40	13.1	1024.19	57.5	2020-10-29 10: 01
3	70.6	125.9	10.5	1.40	13.3	1024.35	57.2	2020-10-29 10: 02
4	71.7	129.2	10.4	1.47	13.3	1024.12	57.7	2020-10-29 10: 03
5	81	142.4	10.3	1.39	13.2	1024.33	58.4	2020-10-29 10: 04
6	74.8	136.4	10.2	1.26	13.5	1024.43	56.1	2020-10-29 10: 05
7	69.9	133.3	10.2	1.09	13.5	1024.42	56.4	2020-10-29 10: 06
8	73.9	130	10.2	1.08	13.5	1024.13	55.8	2020-10-29 10: 07
9	74.9	151.2	10.4	1.31	13.6	1024.22	55.2	2020-10-29 10: 08
10	71.7	132.1	10.5	1.34	13.6	1024.02	55.4	2020-10-29 10: 09
11	76.9	158.3	10.7	1.11	13.6	1024.16	54.9	2020-10-29 10: 10

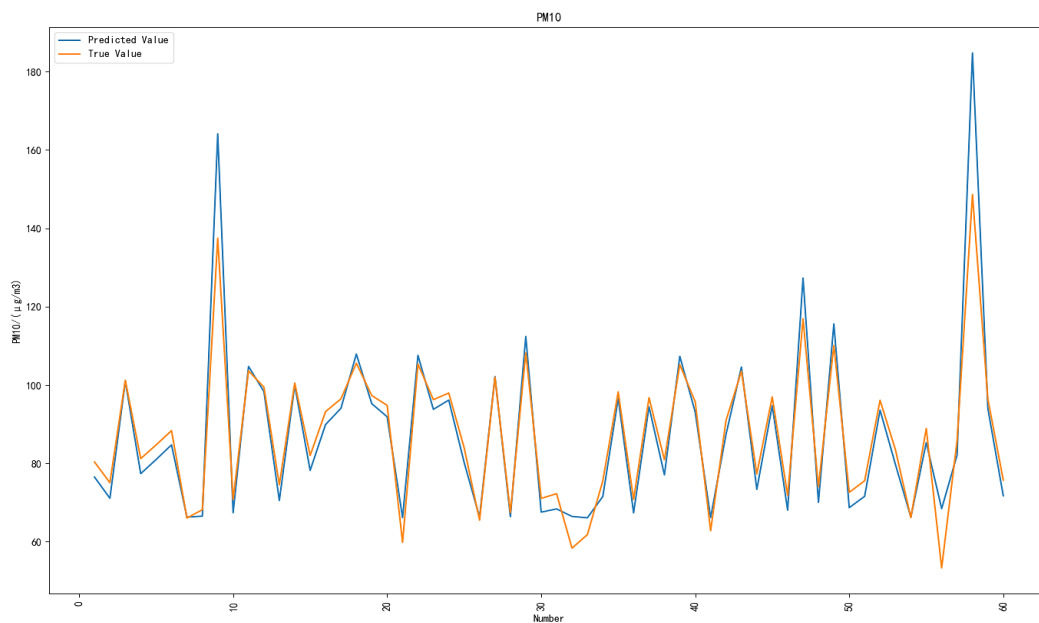
12	76.8	137.3	11.0	1.13	13.6	1024.31	55	2020-10-29 10: 11
13	70.5	133.5	10.8	1.07	13.4	1024.53	55.6	2020-10-29 10: 12
...
1496	65.35	113.1	13.04	2.13	16.89	1019.01	50.62	2020-11-13 14: 55
1497	67.25	117.3	13.12	2.13	16.89	1019.01	50.6	2020-11-13 14: 56
1498	65.75	114.05	13.23	2.09	16.89	1019.01	50.63	2020-11-13 14: 57
1499	65.3	114.2	13.24	2.44	13.22	1019.61	50.82	2020-11-13 14: 58
1500	64.25	107.95	13.27	2.43	13.22	1019.61	51.02	2020-11-13 14: 59

4.2. Data Analysis

The highway construction subgrade-filling process was selected, where road construction-dust monitoring and meteorological factor data were used as the original data. Based on the DNN algorithm, PM2.5 and PM10 concentrations in the highway subgrade-filling construction dust were predicted. In this study, the first 80% of the monitoring data obtained from a fixed point was selected as the training set, and the final 20% as the test set. The predicted and actual values of PM2.5 and PM10 concentrations were compared, as shown in Figure 6.



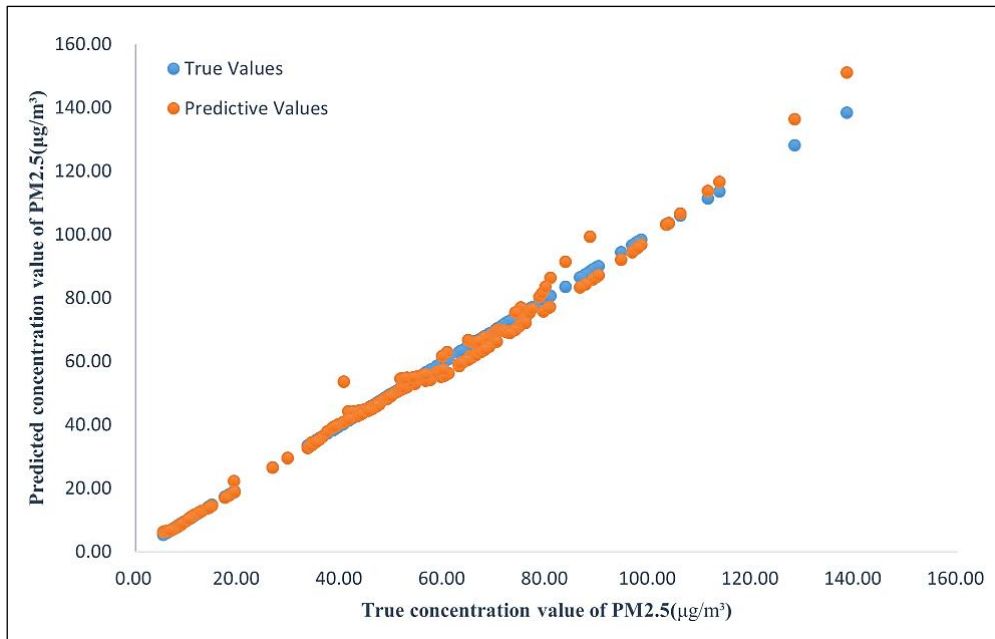
(a) Actual and predicted PM2.5 concentrations



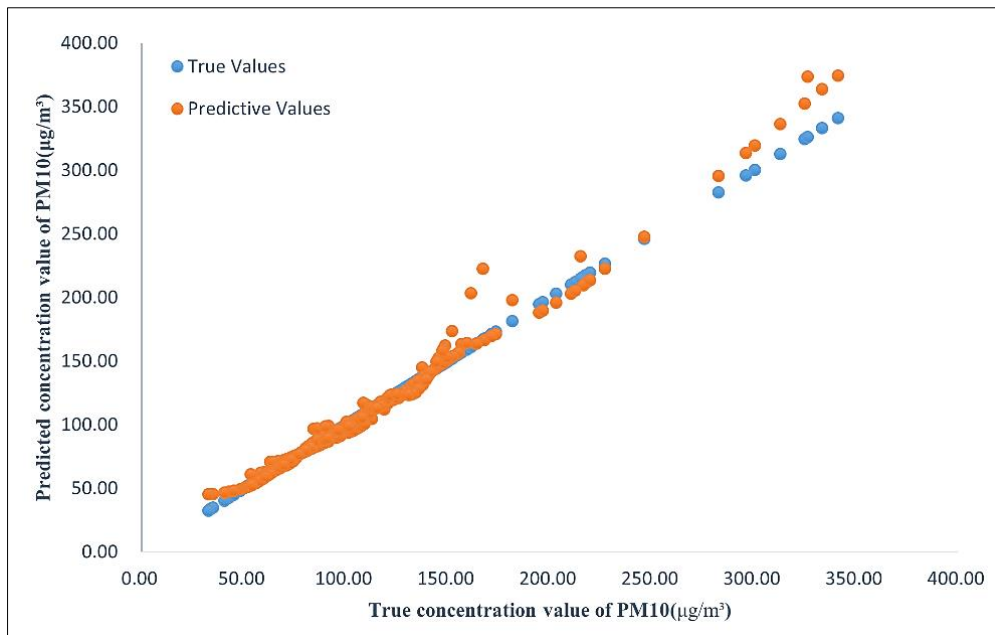
(b) Actual and predicted PM10 concentrations

Figure 6. Comparison between predicted and actual values of PM2.5 and PM10 concentrations

The fitting relationship between the predicted and actual values of PM2.5 and PM10 concentrations in the model test set is shown in Figure 7.



(a) Fitting graph of predicted and actual PM2.5 concentrations in test set



(b) Fitting graph of predicted and actual PM10 concentration in test set

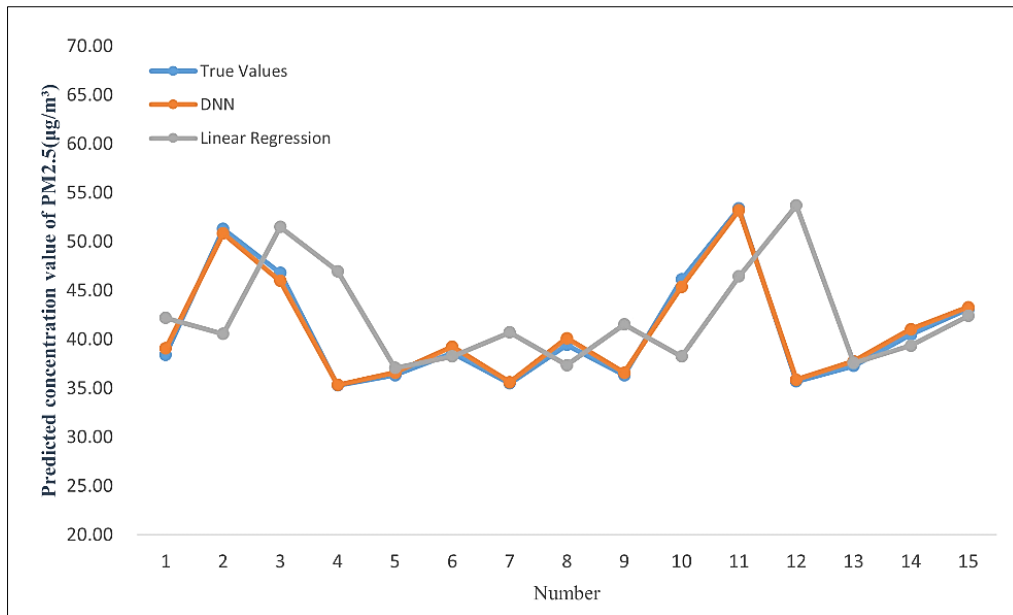
Figure 7. Fitting graph between predicted and actual PM2.5 and PM10 concentrations in test set

The predicted values were compared with the actual values, and an error analysis was performed to verify the accuracy of the DNN-based dust prediction model for highway subgrade-filling construction. The MAPE and RMSE were selected for error analysis. The error calculation results for the test set obtained using Equations 5 and 6 are listed in Table 3.

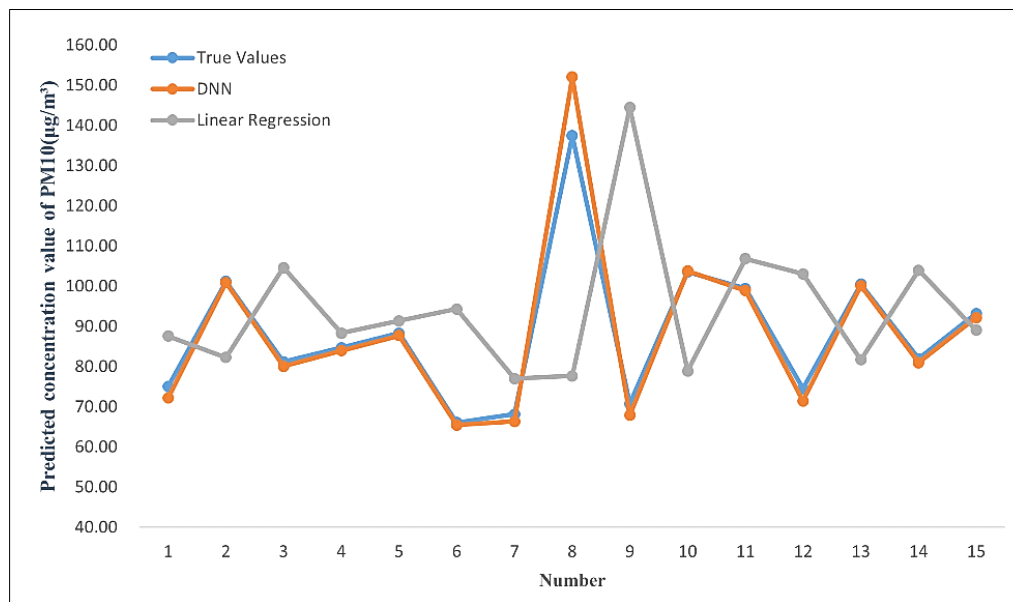
Table 3. Error calculation results for test set

	MAPE (%)	RMSE
PM2.5	1.0427	0.6591
PM10	2.5304	1.4845

A comparison of the error transmission effect between the linear regression and DNN models is shown in Figure 8.



(a) Comparison of PM2.5 concentrations obtained using different methods



(a) Comparison of PM2.5 concentrations obtained using different methods

Figure 8. Comparison between predicted and actual values obtained using different methods

In summary, the DNN model exhibited better prediction performance for dust emissions during highway subgrade-filling construction than the linear regression model. The DNN-predicted values of PM2.5 and PM10 concentrations exhibited a trend similar to that of the actual values; the RMSE between the predicted and actual values was small; and the MAPE was approximately zero. The accuracy and effectiveness of the proposed model were verified. However, significant differences were observed between the predicted and actual values for some data peaks. The analysis results revealed four reasons contributing to the peak value: ① meteorological factors, such as wind and dry climate, which increased the dust content; ② mechanical factors, such as vehicles driving through, which contributed to dust settling on the ground; ③ operational factors, such as earthwork backfilling as well as loading and unloading of soil materials in subgrade filling; ④ process factors, such as paving, leveling, and rolling.

The accurate prediction of highway construction dust data will allow the appropriate measures to be initiated timely to reduce dust concentrations and ensure orderly construction and progress.

5. Conclusion

This study demonstrated that the DNN model outperformed conventional linear regression models in predicting fugitive-dust emissions. This superiority can be attributed to the capability of the DNN to capture complex nonlinear relationships between environmental factors and fugitive-dust emission concentrations. Additionally, results showed that the MAPE and RMSE between the predicted and measured PM_{2.5} values of this model were 1.0427 and 0.6591, whereas those between the predicted and measured PM₁₀ values were 2.5304 and 1.4845, respectively, thus indicating a minimal error. This high level of accuracy is crucial for practical applications of the model in highway engineering.

The findings of this study corroborate the notion presented in related studies, i.e., a correlation exists between fugitive construction dust concentrations and meteorological factors. Moreover, the prediction of fugitive construction-dust concentration was confirmed to be a nonlinear multivariate issue with strong coupling among the influencing factors. While ensuring the accuracy of the predicted results, this study addressed the disadvantages of previous prediction models, which could neither effectively perform nonlinear modeling nor capture the relationship between fugitive-dust concentration and monitoring factors. Consequently, engineering managers can implement targeted measures to reduce fugitive-dust generation, such as by adjusting the frequency of water spraying, cleaning construction vehicles, and enclosing waste-transportation vehicles. This would reduce fugitive-dust concentrations at construction sites and promote the sustainable development of highway construction. However, the real-time monitoring and feedback capabilities of DNN models are currently insufficient and require further improvement.

In the future, the DNN model can be extended to other construction scenarios and incorporated with a broader range of environmental indicators to further refine its predictive power. Additionally, one should examine the potential for integrating real-time data acquisition and analysis using the DNN model to enhance the dynamism of dust-management strategies at construction sites.

In summary, our observations validated the effectiveness of the DNN model for predicting fugitive dust emissions during roadbed filling in highway construction. The ability of the DNN model to manage complex nonlinear relationships renders it an effective tool for environmental management in the construction industry. The findings of this study are crucial for reducing fugitive construction dust and advocating green construction practices.

6. Declarations

6.1. Author Contributions

Conceptualization, Z.W. and X.W.; methodology, L.F.; software, Y.L.; validation, Q.D., Y.L., and L.Z.; formal analysis, L.Z.; investigation, Y.L.; resources, L.F.; data curation, X.W.; writing—original draft preparation, Z.W. and X.W.; writing—review and editing, L.Z.; visualization, Q.D.; supervision, Z.W.; project administration, Z.W.; funding acquisition, Z.W. All authors have read and agreed to the published version of the manuscript.

6.2. Data Availability Statement

The data presented in this study are available on request from the corresponding author.

6.3. Funding

This research was funded by Taihang Urban and Rural construction Group Company Limited (Research on Key Technologies of Intelligent Site Construction in Highway Engineering).

6.4. Institutional Review Board Statement

Not applicable.

6.5. Informed Consent Statement

Not applicable.

6.6. Declaration of Competing Interest

The authors declare that they have no known competing financial interests or personal relationships that could have appeared to influence the work reported in this paper.

7. References

- [1] Lin, Y., & Huang, J. (2021). Can highway networks promote productivity? Evidence from China. *Journal of Advanced Transportation*, 2021(1), 6860979. doi:10.1155/2021/6860979.
- [2] Meng, J., Liu, J., Fan, S., Kang, C., Yi, K., Cheng, Y., Shen, X., & Tao, S. (2016). Potential health benefits of controlling dust emissions in Beijing. *Environmental Pollution*, 213, 850–859. doi:10.1016/j.envpol.2016.03.021.

- [3] Ngoc, L. T. N., Park, D., Lee, Y., & Lee, Y. C. (2017). Systematic review and meta-analysis of human skin diseases due to particulate matter. *International Journal of Environmental Research and Public Health*, 14(12), 1458. doi:10.3390/ijerph14121458.
- [4] Kim, H. B., Shim, J. Y., Park, B., & Lee, Y. J. (2018). Long-term exposure to air pollutants and cancer mortality: A meta-analysis of cohort studies. *International Journal of Environmental Research and Public Health*, 15(11), 2608. doi:10.3390/ijerph15112608.
- [5] Kowalska, M., Skrzypek, M., Kowalski, M., Cyrus, J., Ewa, N., & Czech, E. (2019). The relationship between daily concentration of fine particulate matter in ambient air and exacerbation of respiratory diseases in Silesian agglomeration, Poland. *International Journal of Environmental Research and Public Health*, 16(7), 1131. doi:10.3390/ijerph16071131.
- [6] Sanyal, S., Rochereau, T., Maesano, C. N., Com-Ruelle, L., & Annesi-Maesano, I. (2018). Long-term effect of outdoor air pollution on mortality and morbidity: A 12-year follow-up study for metropolitan France. *International Journal of Environmental Research and Public Health*, 15(11), 2487. doi:10.3390/ijerph15112487.
- [7] Wen, J. Research and analysis on manual monitoring and online monitoring of dust in construction site. *Environment and Development*, 32(6), 2. doi:10.16647/j.cnki.cn15-1369/X.2020.06.080.
- [8] Xiao, H., Yang, X., Wu, Q., Bai, Q., Cheng, H., Chen, X., Xue, R., Du, M., Huang, L., Wang, R., & Wang, H. (2019). Estimate emissions of construction fugitive dust in Xi'an. *Acta Scientiae Circumstantiae*, 39(1), 222–228. doi:10.13671/j.hjkxxb.2018.0377.
- [9] Limsawasd, C., & Athigakunagorn, N. (2022). Quantification of Particulate Emission from Construction Activities Using Discrete-Event Simulation. *Civil Engineering and Architecture*, 10(2), 703–714. doi:10.13189/cea.2022.100225.
- [10] Stevulova, N., Estokova, A., Holub, M., Singovszka, E., & Csach, K. (2020). Characterization of demolition construction waste containing asbestos, and the release of fibrous dust particles. *Applied Sciences (Switzerland)*, 10(11), 4048. doi:10.3390/app10114048.
- [11] Hou, Y., Xing, M., Pan, Y., & Li, S. Analysis of dust emission characteristics and key influencing factors of construction sites in Beijing earthwork stage. *Environmental Pollution and Control*, 02, 171–177 181. doi:10.15985/j.cnki.1001-3865.2021.02.007.
- [12] Huang, Y. H., Tian, G., Qin, J. P., Li, G., & Yan, B. L. (2007). Characteristics of fugitive dust pollution in different construction phases. *Huanjing Kexue/Environmental Science*, 28(12), 2885–2888. doi:10.3321/j.issn:0250-3301.2007.12.038.
- [13] Zhang, L. K., Li, L. J., Jiang, L., Zhao, W. H., Lu, H. F., Wang, X. H., & Qiu, Y. (2019). Spatial and Temporal Distribution Characteristics and Fugitive Dust Emission of Building Sites in Beijing. *Huanjing Kexue/Environmental Science*, 40(1), 135–142. doi:10.13227/j.hjkx.201804236.
- [14] Liang, S., Fu, Q., Liu, Q., Xu, J., Yin, Y., Chen, X., & Cheng, J. Dust pollution characteristics of typical construction sites in autumn in Shanghai during construction stage. *Environmental Pollution and Control*, 12, 1394–1399. doi:10.15985/j.cnki.1001-3865.2018.12.014.
- [15] Van Deurssen, E., Pronk, A., Spaan, S., Goede, H., Tielemans, E., Heederik, D., & Meijster, T. (2014). Quartz and respirable dust in the Dutch construction industry: A baseline exposure assessment as part of a multidimensional intervention approach. *Annals of Occupational Hygiene*, 58(6), 724–738. doi:10.1093/annhyg/meu021.
- [16] Li, X., Su, S., & Huang, T. Quantitative evaluation of construction dust health damage. *Journal of Tsinghua University*, 01, 50–55. doi:10.16511/j.cnki.qhdxxb.2015.01.009.
- [17] Guo, P., Tian, W., & Li, H. (2022). Dynamic health risk assessment model for construction dust hazards in the reuse of industrial buildings. *Building and Environment*, 210. doi:10.1016/j.buildenv.2021.108736.
- [18] Tjoe Nij, E., Hilhorst, S., Spee, T., Spierings, J., Steffens, F., Lumens, M., & Heederik, D. (2003). Dust control measures in the construction industry. *Annals of Occupational Hygiene*, 47(3), 211–218. doi:10.1093/annhyg/meg023.
- [19] Gao, Y., Huo, J., Jia, X., & Wu, G. Research into dust monitoring and measures of construction sites based on big data. *Building Structure*, S1, 1003–1007. doi:10.19701/j.jzjg.2019.S1.215.
- [20] Ma, G., Han, Y., Lu, J., Yao, J., & S, Y. Design and implementation of automatic monitoring system for constructional fugitive dust pollution sources based on UAV. *Environmental Monitoring in China*, 01, 151–156. doi:10.19316/j.issn.1002-6002.2018.01.21.
- [21] Liu, C., Henderson, B. H., Wang, D., Yang, X., & Peng, Z. R. (2016). A land use regression application into assessing spatial variation of intra-urban fine particulate matter (PM_{2.5}) and nitrogen dioxide (NO₂) concentrations in City of Shanghai, China. *Science of the Total Environment*, 565, 607–615. doi:10.1016/j.scitotenv.2016.03.189.
- [22] Eeftens, M., Tsai, M. Y., Ampe, C., Anwander, B., Beelen, R., Bellander, T., Cesaroni, G., Cirach, M., Cyrus, J., de Hoogh, K., De Nazelle, A., de Vocht, F., Declercq, C., Dedele, A., Eriksen, K., Galassi, C., Gražulevičiene, R., Grivas, G., Heinrich, J., ... Hoek, G. (2012). Spatial variation of PM_{2.5}, PM₁₀, PM_{2.5} absorbance and PM_{coarse} concentrations between and within 20 European study areas and the relationship with NO₂ - Results of the ESCAPE project. *Atmospheric Environment*, 62, 303–317. doi:10.1016/j.atmosenv.2012.08.038.

- [23] Tai, A. P. K., Mickley, L. J., & Jacob, D. J. (2010). Correlations between fine particulate matter (PM_{2.5}) and meteorological variables in the United States: Implications for the sensitivity of PM_{2.5} to climate change. *Atmospheric Environment*, 44(32), 3976–3984. doi:10.1016/j.atmosenv.2010.06.060.
- [24] Pateraki, S., Asimakopoulos, D. N., Flocas, H. A., Maggos, T., & Vasilakos, C. (2012). The role of meteorology on different sized aerosol fractions (PM₁₀, PM_{2.5}, PM_{2.5-10}). *Science of the Total Environment*, 419, 124–135. doi:10.1016/j.scitotenv.2011.12.064.
- [25] Zhang, Z., Zhang, X., Gong, D., Quan, W., Zhao, X., Ma, Z., & Kim, S. J. (2015). Evolution of surface O₃ and PM_{2.5} concentrations and their relationships with meteorological conditions over the last decade in Beijing. *Atmospheric Environment*, 108, 67–75. doi:10.1016/j.atmosenv.2015.02.071.
- [26] Zhang, C., Ni, Z., & Ni, L. (2015). Multifractal detrended cross-correlation analysis between PM_{2.5} and meteorological factors. *Physica A: Statistical Mechanics and Its Applications*, 438, 114–123. doi:10.1016/j.physa.2015.06.039.
- [27] Li, B., Zhang, W., & Lu, M. (2018). Multiple linear regression haze-removal model based on dark channel prior. 2018 International Conference on Computational Science and Computational Intelligence (CSCI), 307–312. doi:10.1109/CSCI46756.2018.00066.
- [28] Liu, S., Luo, Q., Feng, M., Zhou, L., Qiu, Y., Li, C., ... & Yang, F. (2023). Enhanced nitrate contribution to light extinction during haze pollution in Chengdu: Insights based on an improved multiple linear regression model. *Environmental Pollution*, 323, 121309. doi:10.1016/j.envpol.2023.121309.
- [29] Nichiforov, C., Stamatescu, I., Fagarasan, I., & Stamatescu, G. (2017). Energy consumption forecasting using ARIMA and neural network models. *Proceedings - 2017 5th International Symposium on Electrical and Electronics Engineering, ISEEE 2017*, 2017-December, 1–4. doi:10.1109/ISEEE.2017.8170657.
- [30] Cabaneros, S. M., Calautit, J. K., & Hughes, B. R. (2019). A review of artificial neural network models for ambient air pollution prediction. *Environmental Modelling and Software*, 119, 285–304. doi:10.1016/j.envsoft.2019.06.014.
- [31] Fauzi, F., Wasono, R., & Kharisudin, I. (2023). Evaluating Recurrent Neural Networks and Long Short-Term Memory for Air Pollution Forecasting: Mitigating the Impact of Volatile Environmental Factors. *Communications in Mathematical Biology and Neuroscience*, 2023, 129. doi:10.28919/cmbn/8265.
- [32] Chen, Q., Ding, R., Mo, X., Li, H., Xie, L., & Yang, J. (2024). An adaptive adjacency matrix-based graph convolutional recurrent network for air quality prediction. *Scientific Reports*, 14(1), 4408. doi:10.1038/s41598-024-55060-2.
- [33] Elshaboury, N., Mohammed Abdelkader, E., & Al-Sakkaf, A. (2023). Convolutional neural network-based deep learning model for air quality prediction in October city of Egypt. *Construction Innovation*. doi:10.1108/CI-11-2022-0292.
- [34] Bedi, S., Katiyar, A., Krishnan, N. M. A., & Kota, S. H. (2024). Utilizing LSTM models to predict PM_{2.5} levels during critical episodes in Delhi, the world's most polluted capital city. *Urban Climate*, 53, 101835. doi:10.1016/j.uclim.2024.101835.
- [35] Wen, D., Zheng, S., Chen, J., Zheng, Z., Ding, C., & Zhang, L. (2023). Hyperparameter-Optimization-Inspired Long Short-Term Memory Network for Air Quality Grade Prediction. *Information (Switzerland)*, 14(4), 243. doi:10.3390/info14040243.
- [36] Wang, Z., Feng, J., Fu, Q., Gao, S., Chen, X., & Cheng, J. (2019). Quality control of online monitoring data of air pollutants using artificial neural networks. *Air Quality, Atmosphere and Health*, 12(10), 1189–1196. doi:10.1007/s11869-019-00734-4.
- [37] Araujo, L. N., Belotti, J. T., Alves, T. A., Tadano, Y. de S., & Siqueira, H. (2020). Ensemble method based on Artificial Neural Networks to estimate air pollution health risks. *Environmental Modelling and Software*, 123, 104567. doi:10.1016/j.envsoft.2019.104567.
- [38] Karacan, C. Ö. (2009). Forecasting gob gas venthole production performances using intelligent computing methods for optimum methane control in longwall coal mines. *International Journal of Coal Geology*, 79(4), 131–144. doi:10.1016/j.coal.2009.07.005.
- [39] Karacan, C. Ö. (2008). Modeling and prediction of ventilation methane emissions of U.S. longwall mines using supervised artificial neural networks. *International Journal of Coal Geology*, 73(3–4), 371–387. doi:10.1016/j.coal.2007.09.003.
- [40] Mathatho, S., Owolawi, P. A., & Tu, C. (2019). Prediction of methane levels in underground coal mines using artificial neural networks. *IcABCD 2019 - 2nd International Conference on Advances in Big Data, Computing and Data Communication Systems*, 1–4. doi:10.1109/ICABCD.2019.8851041.
- [41] Park, S., Kim, M., Kim, M., Namgung, H. G., Kim, K. T., Cho, K. H., & Kwon, S. B. (2018). Predicting PM₁₀ concentration in Seoul metropolitan subway stations using artificial neural network (ANN). *Journal of Hazardous Materials*, 341, 75–82. doi:10.1016/j.jhazmat.2017.07.050.
- [42] Li, X., Peng, L., Yao, X., Cui, S., Hu, Y., You, C., & Chi, T. (2017). Long short-term memory neural network for air pollutant concentration predictions: Method development and evaluation. *Environmental Pollution*, 231, 997–1004. doi:10.1016/j.envpol.2017.08.114.

- [43] Wu, Q., & Lin, H. (2019). A novel optimal-hybrid model for daily air quality index prediction considering air pollutant factors. *Science of the Total Environment*, 683, 808–821. doi:10.1016/j.scitotenv.2019.05.288.
- [44] Karim, F., Majumdar, S., Darabi, H., & Chen, S. (2017). LSTM Fully Convolutional Networks for Time Series Classification. *IEEE Access*, 6, 1662–1669. doi:10.1109/ACCESS.2017.2779939.
- [45] Yousif, J. H., Kazem, H. A., & Bwalya, K. J. (2024). Dust impact on photovoltaic technologies: a comparative analysis using deep recurrent neural networks. *Energy Sources, Part A: Recovery, Utilization and Environmental Effects*, 46(1), 3023–3040. doi:10.1080/15567036.2024.2310740.
- [46] Huang, C. J., & Kuo, P. H. (2018). A deep CNN-LSTM model for particulate matter (PM2.5) forecasting in smart cities. *Sensors (Switzerland)*, 18(7), 2220. doi:10.3390/s18072220.
- [47] Wu, C., Li, Q., Hou, J., Karimian, H., & Chen, G. (2018). PM2.5 concentration prediction using convolutional neural networks. *Magnetic Protostars and Planets (MAPP)*, 43, 68–75. doi:10.16251/j.cnki.1009-2307.2018.08.011.
- [48] Gu, Y., Li, B., & Meng, Q. (2023). Multi-task Deep Neural Network for Air Pollution Prediction and Spatial Effect Analysis. *2023 8th International Conference on Cloud Computing and Big Data Analytics, ICCCBDA 2023*, 220–227. doi:10.1109/ICCCBDA56900.2023.10154688.
- [49] Kek, H. Y., Bazgir, A., Tan, H., Lee, C. T., Hong, T., Othman, M. H. D., Fan, Y. Van, Mat, M. N. H., Zhang, Y., & Wong, K. Y. (2024). Particle dispersion for indoor air quality control considering air change approach: A novel accelerated CFD-DNN prediction. *Energy and Buildings*, 306, 113938. doi:10.1016/j.enbuild.2024.113938.